# Linear-dichroism studies of thin Dy overlayers on Ni(110) and Cu(110) substrates

R. J. H. Kappert and J. Vogel
*Spectroscopies of Solids and Surfaces, Research Institute for Materials, University of Nijmegen, Toernooiveld, NL-6525 ED Nijmegen, The Netherlands*

M. Sacchi
*Laboratoire pour l'Utilisation du Rayonnement Électromagnétique, Commissariat à l'Energie Atomique and Ministère de l'Education Nationale, Université Paris-Sud, Bâtiment 209d, 91405 Orsay CEDEX, France*

J. C. Fuggle*
*Spectroscopies of Solids and Surfaces, Research Institute for Materials, University of Nijmegen, Toernooiveld NL-6525 ED Nijmegen, The Netherlands*

(Received 11 November 1992; revised manuscript received 9 February 1993)

In this paper we present polarization-, temperature-, and thickness-dependent x-ray-absorption measurements on extremely thin Dy overlayers. For Dy overlayers deposited at room temperature on Cu(110) and (magnetic) Ni(110) we observe strong linear dichroism. We deduce that the nature of the dichroic effects is predominantly electrostatic. When Dy is evaporated onto Ni(110) and kept at 50 K almost no dichroism is observed. Deposition of Dy on Cu(110) at 50 K, on the other hand, yields strong dichroism. We discuss these effects in greater detail and formulate a model for the overlayer system that seeks to explain the observed differences. Finally, a strong decrease of dichroism is observed as the Dy layer thickness increases, a phenomenon which is independent of the substrate. We propose a mechanism to explain this that involves counteracting contributions to the dichroism from both the overlayer-substrate and surface-vacuum interfaces. We illustrate this with an experiment involving a Ho probing layer.

## I. INTRODUCTION

Dichroism is an old technique that dates back to its discovery by Zeeman.[1] In the 1970s, predictions on[2] and subsequent search for[3] magneto-optical effects opened the way for the discovery of very large magnetic x-ray dichroism (MXD).[4,5] MXD has since been the subject of many investigations, both experimental[6–17] and theoretical.[18–29]

Using *linearly* polarized light, strong dichroic effects are expected (and observed) in the $3d \rightarrow 4f$ absorption ($M_{4,5}$) spectra of the rare earths (RE's).[4,5,18] This was first demonstrated on a magnetically saturated RE iron garnet,[5] but soon after this, a series of experiments using thin RE layers on Ni(110) (Refs. 6, 9, and 30) and Si(111) substrates[10] were performed also showing large dichroic effects. Most early studies were performed on magnetic substrates, but the observation of strong dichroism in the x-ray-absorption spectra of RE's on Si(111) strengthened the suspicions that the dichroism observed in these thin RE overlayers was actually due to crystal-field effects, rather than originating from magnetic sources. In the course of the present paper we will show that for Dy overlayers in Ni(110) and Cu(110) this is indeed the case. Moreover, we will discuss the influence of the substrate in detail and present a model describing the origin of the dichroic effects.

Dichroism is the dependence of the absorption process on the polarization of the incident light. In x-ray-absorption spectroscopy (XAS) this light causes a transition of a core electron into the unoccupied states, which is governed by the dipole selection rules. If the light is polarized, the selection rules act to favor certain transitions, e.g., with circularly polarized light, the excited electrons are spin polarized.[31]

A special situation occurs for the RE $3d \rightarrow 4f$ edges, where both initial and final states of the absorption process are localized. As a result of the strong localization the absorption process can essentially be described as an atomic process, whereby the transitions from the Hund's rule ground state $3d^{10}4f^n(J)$ to the numerous dipole-allowed final states $3d^9 4f^{n+1}(J')$ are well described by atomic Hartree-Fock calculations. For these edges, strong dichroic effects were predicted for both linearly and circularly polarized light.[4]

One may visualize the process as follows. The transitions can be divided into three groups of spectral lines with $\Delta J = J' - J = +1, 0, -1$ (see Fig. 1, lower part). These groups are generally well separated in energy, and are thus observable as distinct features in the spectrum.[18,30] Except for the dotted spectrum in the upper part of the figure, the spectra depicted in Fig. 1 are calculated by atomic Hartree-Fock theory.[32] The electron correlations of the $4f$ electrons are taken into account by reducing the Hartree-Fock values of the Coulomb and exchange integrals (the so-called Slater integrals) in the de-

 

termination of the multiplet structure.[32] Optimizing the Slater integral reductions and the lifetime and instrumental broadenings[33] the agreement with the isotropic spectrum was good (top spectrum of Fig. 1).

In the presence of a magnetic field, the degenerate ground state will split into $2J + 1$ sublevels $M_J = -J, \ldots, +J$. The relative population of these sublevels is determined by a Boltzmann distribution.[18] At low temperatures, with the thermal energy much smaller than the magnetic splitting, only the lowest-lying Zeeman level ($M_J = -J$) is significantly occupied. Also, the final states are split by the magnetic field. However, the splittings of initial and final states, which are of the order of meV, cannot be resolved due to the core-hole lifetime and instrumental broadenings, which are of the order of 1 eV.

The polarization dependence of the XAS process can now be used to overcome this: if the polarization vector of the incident x rays ($\boldsymbol{E}$) is parallel to the magnetic field ($\boldsymbol{H}$), only transitions with $\Delta M_J = 0$ are allowed, while for $\boldsymbol{E}$ perpendicular to $\boldsymbol{H}$ only transitions with $\Delta M_J = \pm 1$ are allowed. (Using circularly polarized light, the latter transitions can be resolved into $\Delta M_J = +1$ and $\Delta M_J = -1$ transitions, depending on the helicity of the light.[30,33]) The transitions building up the $\Delta J$ groups are dominated by certain $\Delta M_J$ transitions. If the RE ground state is split by a magnetic field only, the $\Delta J$ groups consist mainly of $\Delta M_J = -\Delta J$ transitions.[18,30] Therefore, the total absorption strength of each of the $\Delta J$ groups changes with respect to the unpolarized absorption spectrum, as a function of the angle between

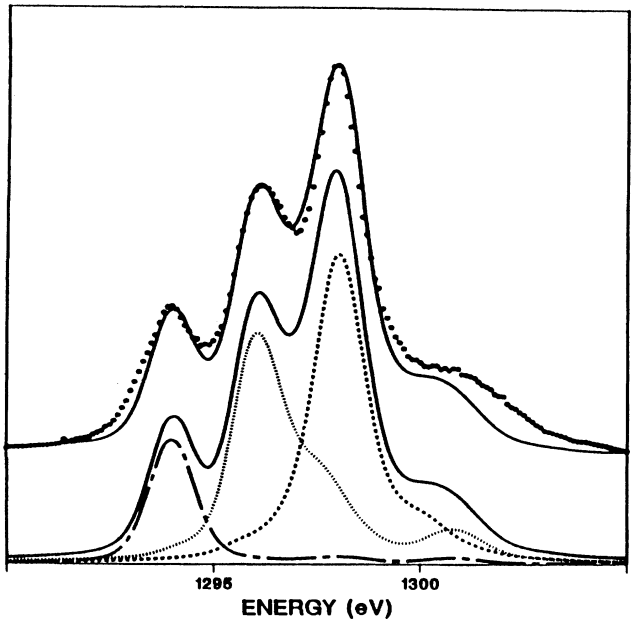


FIG. 1. Top: Isotropic Dy spectrum obtained from a $Dy_3Fe_5O_{12}$ garnet that showed no dichroism (dots) and the theoretical isotropic spectrum (solid line). Bottom: Decomposition of the isotropic spectrum (solid line) into the $\Delta J$ components: $\Delta J = -1$ (dashed line), $\Delta J = 0$ (dotted line), and $\Delta J = +1$ (dash-dotted line). See text for further explanation.

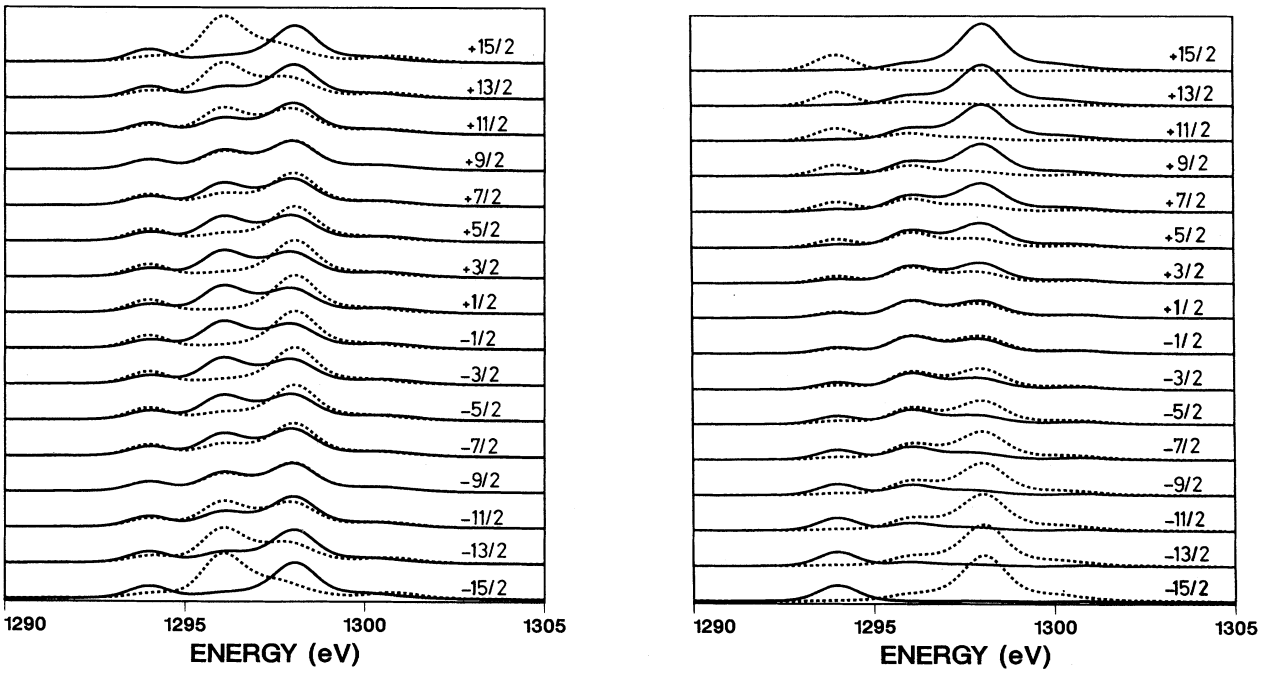


FIG. 2. $T = 0$ K dichroism spectra for $Dy^{3+}$ with linearly (left panel) and circularly (right panel) polarized light. Solid curve: polarization vector perpendicular to the quantization axis (left panel), or left circularly polarized light (right panel). Dashed curve: polarization vector parallel to the quantization axis (left panel), or right circularly polarized light (right panel). The $M_J$ quantum number by which the ground state is characterized is indicated in the figure.

polarization vector and magnetic field vector. The $\Delta J$ groups are well separated in energy, leading to immediately visible changes in the absorption spectrum as the angle of the polarization vector is changed with respect to the magnetic field $\boldsymbol{H}$.

In this paper, we will discuss the influence of electrostatic fields on the x-ray dichroism obtained with linearly polarized light. The reason electrostatic fields can be important for linear dichroism is that linear dichroism is sensitive to $\langle M_J^2 \rangle$, the thermodynamic average of the square of $M_J$, whereas circular dichroism is sensitive to $\langle M_J \rangle$. In the presence of only an electrostatic field all levels of the split ground state are characterized by $\langle M_J \rangle = 0$, leading to absence of circular dichroism, but linear dichroism can still occur. The crystal field (CF) determines the character of the sublevels in the split ground state, which in turn determines the linear dichroism. To illustrate this, we show in Fig. 2 the calculated spectra of $Dy^{3+}$ as a function of $M_J$. The spectra depicted in Fig. 2 are calculated assuming a ground state which consisted of a single $M_J$ level. The $M_J$ number used in the calculation is indicated in the figure. The calculations were performed for $T = 0\,\mathrm{K}$, so that all transitions in the absorption process stem from the indicated level.

The ground state of a Dy ion placed in a pure magnetic field is the $M_J = -15/2$ Zeeman level. Using linearly polarized light, the absorption spectrum obtained for polarization vectors parallel and perpendicular to the magnetization would be markedly different. Note, that the same spectra also occur if a ground state of $M_J = +15/2$ is assumed. In the latter case, however, the left and right circularly polarized XAS spectra would be interchanged with respect to the former case.

Next, consider a simple axial CF, with a ground state

$$|\phi\rangle = \frac{1}{\sqrt{2}}\left(|1/2\rangle + |-1/2\rangle\right) \tag{1}$$

(such a model has been discussed in earlier literature; see Refs. 17 and 30). We conclude from the right panel of Fig. 2 that the sum of the contributions from each $M_J$ leads to an absorption spectrum that is equal for left and right circularly polarized light. From the left panel we observe that for linearly polarized light there still is a difference between the polarization vector perpendicular or parallel to the quantization axis.

The result is that the dichroism for the axial field case resembles that for the magnetic case, albeit with a reversed orientation. We show in Fig. 3 the calculated linear dichroism for Dy, the RE we will report most data on, at $T = 0\,\mathrm{K}$. The left panel shows the calculated spectra for a $Dy^{3+}$ ion in a magnetic field, the right panel the calculated spectra for Dy in the axial field mentioned above. Again, note that the spectra seem "interchanged": the spectrum occurring for the polarization perpendicular to the magnetic field resembles that for the polarization parallel to the axial CF; the spectrum occurring for the polarization parallel to the magnetic field tends more toward the spectrum calculated for the polarization perpendicular to the axial field.

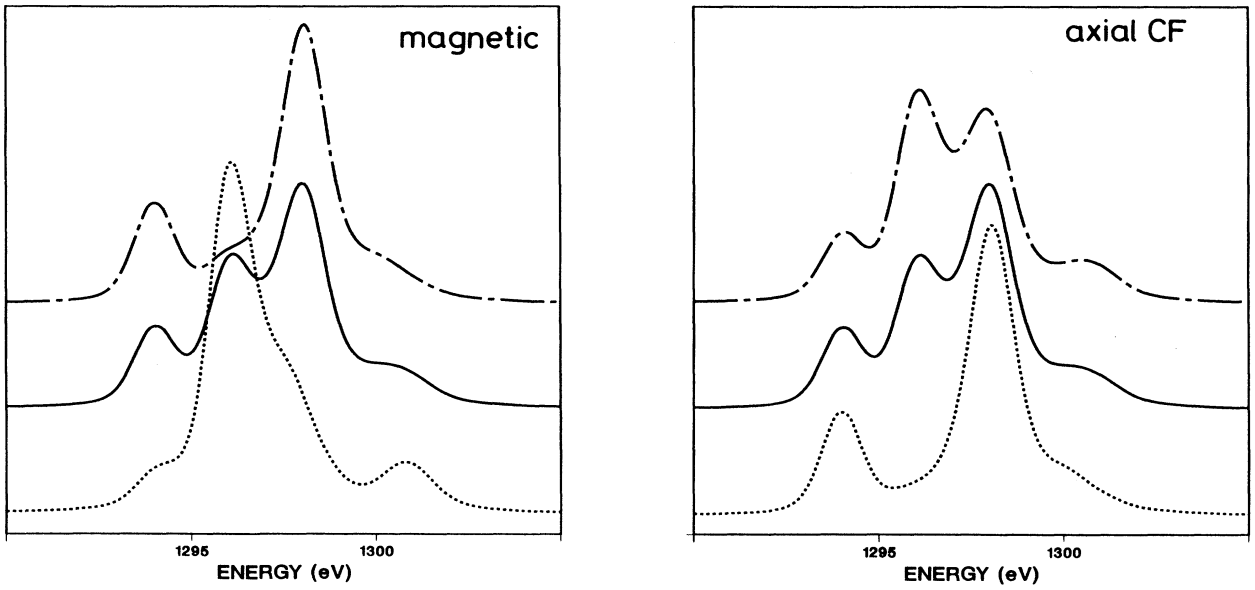


FIG. 3. Calculated dichroism at $T = 0\,\mathrm{K}$. Left panel: magnetic field splitting: isotropic spectrum (solid line), $E$ parallel to magnetization (dotted line), and $E$ perpendicular to the magnetization (dash-dotted line). Right panel: simple axial field splitting: isotropic spectrum (solid line), $E$ parallel to CF (dotted line), and $E$ perpendicular to CF (dash-dotted line). The spectra are normalized on the spectrum for the polarization parallel to the magnetization (left panel, dotted line).

We will also report some data on holmium XAS spectra. The expected Ho $M_5$ spectra are similar to those of Dy. In particular, the dependence of the relative intensities of the three peaks in the Ho spectrum is analogous to those of the peaks in the Dy XAS spectrum. The linear dichroism manifests itself in the relative intensity of the middle peak (which occurs at $\sim$ 1352.5 eV).

We will end this section by noting that magnetic and axial CF cases may be regarded as extremes. In general, crystal fields are more complex, and more subtle behavior may occur in the absorption spectra as a function of the angle between polarization vector and quantization axis, and as a function of temperature.[33]

## II. EXPERIMENT

Ni(110) and Cu(110) single crystals were prepared by mechanical polishing using diamond grains down to 0.25 $\mu$m. The crystals were subsequently cut by spark erosion with the long axis parallel to the [111] axis of the fcc structure (the easy magnetization axis of Ni). The crystals were annealed in a $\sim 5 \times 10^{-4}$-mbar hydrogen flow at 650°C for 12 h to remove contaminants (mainly sulphur) from the bulk. The crystal was mounted on a weak iron yoke, clamped by K-type thermocouple wires. The sample could be heated by electron bombardment via a tungsten filament positioned behind the crystal. The sample holder was mounted on the cold finger of a cryostat electrically separated from it by sapphire plates. The cryostat could be cooled with liquid helium and a lowest temperature of approximately 50 K was reached at the surface of the crystal. The thermocouple that was used is well suited to cover the range of temperatures encountered in the experiment, but is somewhat inaccurate at low temperatures, and we estimate the uncertainty of the temperature readout at 50 K to be $\pm$10 K. The cryostat could rotate in ultrahigh vacuum through a differentially pumped rotary feedthrough.

The single crystal was exposed to sputter-anneal cycles once in vacuum ($10^{-10}$-mbar base pressure), and a good low-energy electron diffraction (LEED) pattern was obtained. No *in situ* check of cleanliness was possible, but the cleaning procedures were tested elsewhere and gave a $<5\%$ of a monolayer (ML) contamination (C, O) as judged by x-ray photoemission spectroscopy (XPS), and the LEED results were the same for XPS and XAS systems. We stress that measurements for the overlayers discussed in this paper have all been completed within 1 h after evaporation, unless explicitly stated otherwise.

A pulsed magnetic field—up to $\sim$ 5 kG—could be applied along the [111] direction of the Ni(110) crystal before collecting XAS spectra in zero-field conditions. *Ex situ* magneto-optical Kerr effect (MOKE) measurements showed that the remanent magnetism of the Ni substrate was $90 \pm 5\%$ of the saturation value.

RE overlayers (RE=Dy,Ho) have been evaporated from both a Knudsen cell furnace and tungsten filaments. The rate of evaporation was approximately 1 Å per minute, while the sample was held at room temperature, or at a constant temperature of 50 K. In the latter case, the sample was cooled down and flash-annealed before evaporation to minimize contamination. During annealing and evaporation the base pressure of $1\times10^{-10}$ mbar rose to $1\times10^{-9}$ mbar. Throughout this paper, when talking about a monolayer we mean the mass equivalent of a single layer of the hcp lattice of the RE, which has a thickness of 2.82 Å. Layer thicknesses were determined with an oscillating quartz crystal monitor. For all RE overlayers the excellent LEED patterns of the single-crystal substrates disappeared upon evaporation, signifying a nonepitaxial growth.

The experiments were carried out on the SA-22 beamline of the Super-ACO positron storage ring, LURE, Orsay.[30] The total instrumental resolution at the $M_5$ edge of Dy is $\sim$ 0.5 eV, which includes the instrumental broadening of the double-crystal monochromator that is equipped with beryl crystals. X rays that are collected are linearly polarized in the plane of the synchrotron. The XAS spectra were obtained in the total electron yield (TEY) mode, where the angle between the sample surface normal and the polarization vector $\boldsymbol{E}$ (denoted $\beta$) was varied between 90° (normal incidence) and 10° (grazing incidence).

## III. Dy OVERLAYERS DEPOSITED AT ROOM TEMPERATURE

The room-temperature $M_5$ XAS spectra of 0.25-ML Dy on a Ni(110) surface are shown in Fig. 4. Between the spectrum obtained at normal incidence ($\beta = 90°$, shown at the top of the figure) and the spectrum taken at grazing incidence ($\beta = 15°$, lower part) the measured $M_5$ edge of Dy in polycrystalline iron garnet ($Dy_3Fe_5O_{12}$) is shown. Because the incident light is linearly polarized, changing the angle of incidence also means changing the polarization vector with respect to the orientation of the Dy ions. We observe from Fig. 4 that the 1296-eV peak changes in intensity as a function of the angle $\beta$, from a minimum intensity at $\beta = 15°$ to a maximum at $\beta = 90°$. Moreover, also the smaller peak at $\sim$ 1294 eV and the high-energy shoulder at $\sim$ 1301 eV change intensity as a function of the orientation of the sample with respect to the polarization vector. We conclude that 0.25-ML Dy on Ni(110) features dichroism.

The spectrum taken from the polycrystalline sample are independent of the angle of incidence. It is the experimental analog of the isotropic spectrum defined previously. This spectrum has been obtained in an earlier study.[9] We note that each individual Dy ion in the polycrystalline sample can experience an asymmetric environment. However, on a macroscopic scale all these asymmetries will average out to give an "isotropic" spectrum (see, e.g., Ref. 33).

To study the influence of magnetic effects on the dichroism spectra we have also studied the (110) surface of Cu. Cu(110) and Ni(110) surfaces are structurally identical but only Ni(110) can be magnetized. In Fig. 5 we present the $M_5$ XAS spectra of 0.5-ML Dy on Cu(110). Again, we observe dichroism, as can be judged from the large difference in the intensity of the 1296-eV peak. There appears to be little difference between the Dy/Ni(110) and Dy/Cu(110) dichroism at room temper-

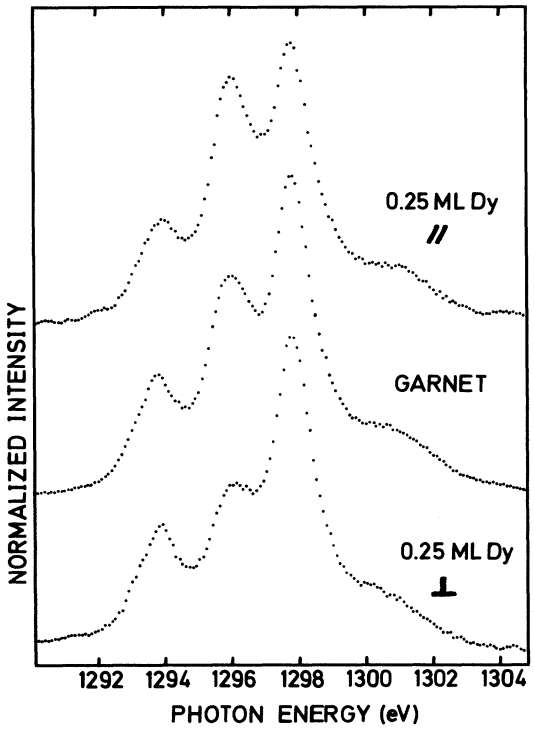


FIG. 4. Experimental Dy $M_5$ XAS spectra, obtained at room temperature, taken from a 0.25-ML Dy on Ni(110). Top spectrum: $E$ parallel to the sample surface. Lower spectrum: $E$ perpendicular to the sample surface. Middle spectrum: experimental spectrum, obtained from a Dy iron garnet ($Dy_3Fe_5O_{12}$), representing a nondichroic spectrum. The figure is taken from Ref. 9; see text.

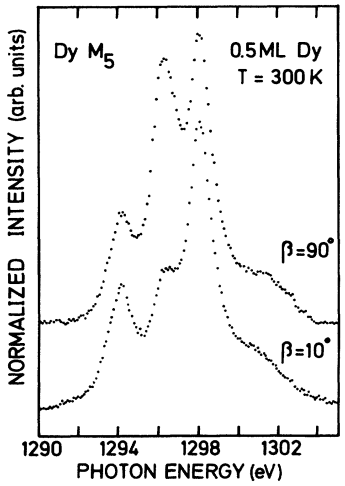


FIG. 5. Dichroism spectra of 0.5-ML Dy on Cu(110). Depicted are the spectra obtained at normal incidence ($\beta = 90°$) and grazing incidence ($\beta = 10°$). The overlayer was deposited and measured at room temperature.

ature, yet the Ni(110) and Cu(110) surfaces are not identical. A noticeable difference is that the Ni(110) surface was magnetized. This gives us an opportunity to discuss the nature of the observed dichroic effects.

First, we note that dichroism is easily observable for Dy on both Ni(110) and Cu(110). This indicates that the Dy ground state is split, and that the occupation of the sublevels of the split ground state is nonuniform. Since the measurements were performed at room temperature we conclude that the total width of the split ground state must be of the order of $kT \approx 25$ meV or larger.

Second, we will demonstrate below that the dichroic effects diminish monotonically as the overlayer thickness increases. Therefore, dichroism does not originate from "bulk" Dy, but is connected with the Dy-substrate interface. We observe that the dichroism of Dy on Cu and Ni substrates is very similar. From this observation we conclude that magnetic fields cannot be the main source of dichroism in these systems. For the magnetically saturated Ni surface magnetic fields may play a role, but for magnetic fields to be the main source of dichroism very large intensities ($> 100$ T) are required at the Dy sites to allow for sufficient ground-state splitting.[33]

We therefore attribute the dichroic effects in the Dy $M_5$ absorption edges to electrostatic fields.[34] This also explains why the dichroism for Dy on Ni(110) was found independent of the remanent magnetization of the Ni(110) crystal.[35]

Angular and temperature dependencies offer further support. The RE $M_{4,5}$ spectra can be analyzed and assigned a value of the dichroism parameter $C$. The $C$ parameter describes the spectrum completely,[18,30,33] and is the product of an angular part ($C_\gamma$) and a term that describes the distribution of the $4f$ electrons over the sublevels in the split ground state, denoted $C_{M_J}$

$$C = C_\gamma C_{M_J} . \tag{2}$$

The angular term is given by the angle $\gamma$ between polarization vector and quantization axis

$$C_\gamma = \tfrac{3}{2}\cos^2\gamma - \tfrac{1}{2} , \tag{3}$$

and $C_{M_J}$ is given by

$$C_{M_J} = \frac{\langle M_J^2\rangle - \frac{1}{3}J(J+1)}{J^2 - \frac{1}{3}J(J+1)} , \tag{4}$$

where $\langle\ \rangle$ denotes the average over the Boltzmann distribution.

We have taken XAS spectra at $\sim 50$ K. From Eqs. (2)–(4) we obtain

$$\frac{C(T)}{C(T')} = \frac{C_\beta C_{M_J}(T)}{C_\beta C_{M_J}(T')} = \frac{\langle M_J^2(T)\rangle - \frac{1}{3}J(J+1)}{\langle M_J^2(T')\rangle - \frac{1}{3}J(J+1)} . \tag{5}$$

for spectra taken at the same angle of incidence. We define the ratio $\eta$:

$$\eta = \frac{C(T = 50\,\mathrm{K})}{C(T = 300\,\mathrm{K})} . \tag{6}$$

From the $C$ values of the room-temperature experiments, we expect $\eta > 2$ for the magnetic and axial CF models.

However, although the dichroic effect does increase upon cooling of the overlayer system, it increases only slightly; we obtain from experiment $\eta \simeq 1.1$.[33] Neither the magnetic model nor the simple axial CF model displayed in Figs. 2 and 3 can be applied satisfactorily to the Dy overlayer system: the effective crystal field affected by the Dy ions must have a symmetry which is different from the axial field discussed so far.

The angular dependencies obtained from freshly deposited Dy layers (open circles) and layers measured more than 4 h after deposition (solid circles) are depicted in Fig. 6 as a function of the measurement angle $\beta$. All spectra have been analyzed, and assigned a $C$ value. There is no dichroism if $C = 0$. This can happen if $C_{M_J} = 0$, i.e., if there is a uniform occupation of the sublevels in the ground state. It is also possible for the dichroism to be zero at the *magic angle* $\gamma_M$ where $C_\gamma = 0$. The magic angle can be seen from Fig. 6 to occur around 55°. Since $\gamma_M = 54.7°$ from Eq. (3), it seems natural to set $\beta = \gamma$. This coincides with the magic angle obtained from the model using an axial CF directed perpendicularly to the surface plane. The magic angle obtained from a model using a magnetic field is $\beta = 90° - 57.4° = 32.6°$, which is at variance with the experimental angular dependence. A model in which the magnetic field is oriented perpendicularly to the surface cannot reconcile the shape of the predicted spectra with those measured. Again, we must conclude that the splitting of the ground state is not due to magnetic interactions. [The angular dependence for Dy on Ni(110) is not shown, but follows the same pattern. In particular, the magic angle is identical to that obtained from Dy/Cu(110).]

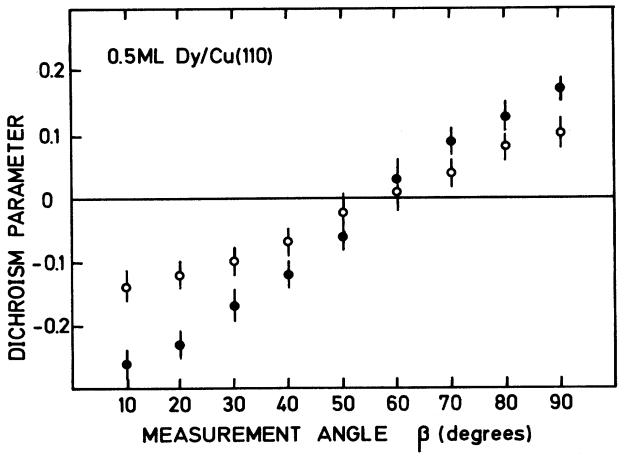


FIG. 6. Angular dependence of the dichroism of 0.5-ML Dy on Cu(110). Depicted is the variation of the dichroism parameter $C$, as determined from the observed spectra, versus the measurement angle $\beta$ that is defined as the angle between the surface normal and the polarization vector. The estimated error in the determination of $C$ is indicated by the sticks. The open circles represent the dichroism observed from a freshly evaporated layer (obtained no later than 1 h after evaporation) and the solid circles represent data from old layers (obtained more than 4 h after evaporation).

## IV. A MODEL FOR THE Dy ADSORPTION

We observe in Fig. 6 a peculiar behavior of the dichroism intensity as a function of time: the longer the Dy overlayer is exposed to the vacuum, the stronger the dichroism becomes. For Dy overlayers on Ni(110) this behavior has not been observed. It is in order to explain this that we have formulated a model, which will be able to make predictions on a qualitative level.

Interdiffusion of substrate and overlayer atoms can influence the dichroism. Not much is known about the rare-earth–transition-metal interdiffusion, and the reported data are confusing. Large diffusion rates of Ni atoms through Gd (Ref. 36) or Yb (Refs. 37 and 38) have been reported. The diffusion has been observed for substrates as cold as 150 K. However, for Tb overlayers deposited on Ni(111) no interdiffusion was reported for substrate temperatures below 300 K, and Yb overlayers only start alloying with Ni after a critical layer thickness has been reached.[39] For the Cu surface on the other hand, no interdiffusion was reported even at room temperature.[36]

Our model indirectly incorporates interdiffusion processes. The model views the adsorption process as follows. A Dy ion hits the substrate surface. At $T = 0$ K it would stick to the spot it had hit. The Dy ions would experience a wide variety of charge density symmetries, similar to the range of symmetries they would be exposed to in a polycrystalline solid. Consequently, we expect small or no dichroism.

At finite substrate temperatures the Dy ion may have enough energy to overcome the kinetic activation energy and move to an energetically more favorable position. This position may be at the surface or, via an interdiffusion process, below it. If a relatively large number of adsorbate ions occupy such sites the Dy ions will very likely experience a much more uniform environment. This will lead to an enhancement in the dichroism intensity.

Substrates differ in, e.g., the height of the kinetic activation barrier. Substrates with a low kinetic activation barrier allow more mobility of the adsorbate atoms than substrates where this barrier is high.

In terms of this model, the aging phenomenon in Fig. 6 reflects a slow rearrangement of Dy ions on the Cu surface. For Ni, which is more reactive than Cu, such aging phenomena have not been observed since the ions are less able to overcome the energy barrier.

## V. Dy OVERLAYERS DEPOSITED AT LOW TEMPERATURE

In Fig. 7 the spectra that were obtained for a 0.5-ML Dy deposited on a 50-K substrate are shown. Here the sample was kept at 50-K while Dy was evaporated on the sample surface, and the spectra were taken after the evaporation had been completed. From the left panel of Fig. 7 it is obvious that the observed dichroism for Dy overlayers deposited on a 50-K Cu(110) surface are equivalent to those of the overlayers deposited on a room-temperature surface, depicted in Fig. 5 and the spectra obtained from the latter system when cooled down.

If we turn to the results obtained when evaporating Dy

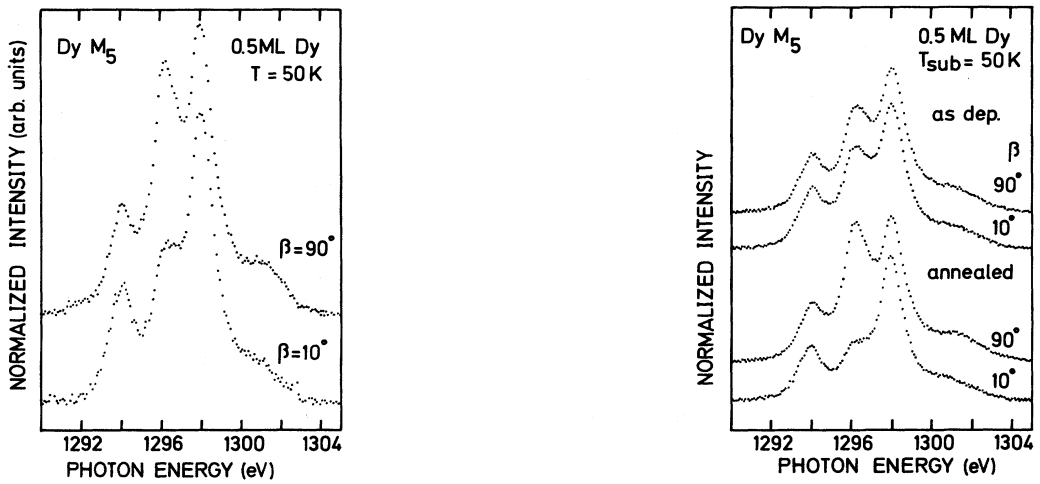


FIG. 7. Dichroism spectra for 0.5-ML Dy on Cu(110) (left panel) and Ni(110) (right panel). Overlayers were deposited and measured at 50 K. Left panel: The top curve was measured at normal incidence ($\beta = 90°$), and the lower curve at grazing incidence ($\beta = 10°$). Right panel: top: spectra of the overlayer at normal incidence ($\beta = 90°$) and grazing incidence ($\beta = 10°$). Bottom: spectra obtained from the Dy overlayer after annealing it for 1 min at 300°C, for $\beta = 90°$ and $\beta = 10°$.

on a 50-K Ni(110) substrate (Fig. 7, right panel, top spectra), we see that, in contrast to the room-temperature measurements, large dichroic effects are not observed. Detailed analysis shows there still is dichroism, but it is much smaller than observed at room temperature. A similar observation has been reported by Sacchi, Sakho, and Rossi for the deposition of Dy on Si(111).[10]

The difference in the dichroism of Dy atoms adsorbed on Ni(110) and Cu(110) at low temperatures can be interpreted in terms of mobility over the surface (see Sec. IV). Ni is more reactive than Cu (e.g., the heat of formation of Ni-Gd alloys is 0.38 eV/atom whereas for Cu-Gd it is 0.25 eV/atom, based on a simple Miedema calculation[36,40]) and Dy atoms are probably more free to move over the Cu surface than over the Ni surface.[41]

The bottom part of the right panel of Fig. 7 shows a strong increase in dichroism as a result of an annealing treatment at 300 °C of the Dy overlayer on Ni(110) deposited and measured at 50 K. Whereas before there was little dichroism, after annealing the dichroism is clearly visible. If we employ the model outlined in Sec. IV, this behavior can be interpreted as a consequence of increased ordering in the overlayer. The higher temperatures during annealing allow the overlayer atoms to relax into a configuration at lower energy. The electronic environment of the overlayer ions will be more uniform, and the dichroism will therefore increase.

## VI. THE ROLE OF THE SURFACE AND THE SUBSTRATE-OVERLAYER INTERFACE

In this section we present a study into the contributions of the substrate-overlayer interface and the surface regions of the overlayer to the total dichroism signal. We were inspired by the observed layer thickness dependence (Fig. 8). The absolute value of $C$ decreases monotonically as the overlayer grows (remember there is no dichroism if $C = 0$). Figure 8 is also representative of the thickness dependence of Tb on Ni(110),[30] Dy on Si(111),[10] and Dy on Cu(110). The origin of this layer thickness dependence is not clear. However, it is clear that the CF felt by the individual Dy atoms is a function of the position in the overlayer: the environment of a Dy ion at the Dy-substrate interface is different from that of a surface Dy ion and of a Dy "bulk" ion.

The Dy atoms in the most asymmetric environment are located at the surface and the substrate-overlayer interface. Let us suppose then that these atoms are responsible for the dichroic effects observed, and that the "bulk" Dy atoms are inactive. Increasing the overlayer

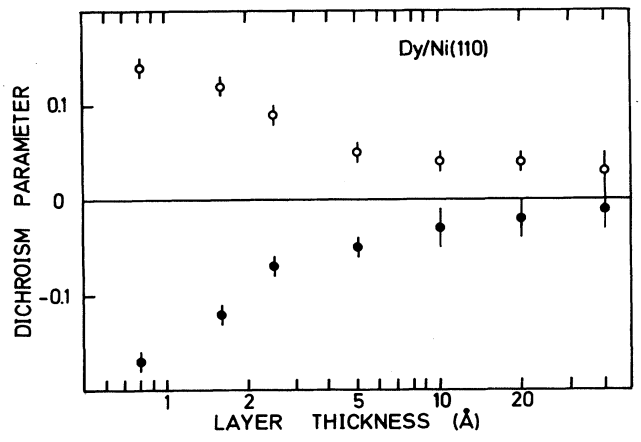


FIG. 8. Layer thickness dependence of the dichroic effect. The dichroism parameter ($C$, see text) of the spectra are plotted versus the layer thickness. Open circles: data obtained at normal incidence (measurement angle $\beta = 90°$). Solid circles: data obtained at grazing incidence ($\beta = 10°$). Estimated uncertainty in the determination of the dichroism parameter is represented by sticks.

thickness would mean decreasing the relative contribution of the active Dy atoms to the total spectrum, thus decreasing the dichroism. The behavior of the dichroism signal as a function of layer thickness as displayed in Fig. 8 then seems understandable. However, the contributions of the active regions need to be studied in more detail.

We have already established that the substrate can have a considerable influence on the dichroism (Sec. V), since it can be responsible for a more uniform environment for the Dy atoms on its surface. We see this reflected again in the spectra of Fig. 9, where a small quantity of Ho was evaporated on top of a larger quantity of Dy.

Since the Dy overlayer does not grow epitaxially, its surface is highly irregular and cannot be expected to induce such large effects as the single-crystal surfaces discussed before. Indeed, the dichroism observed from the Ho $M_5$ XAS spectra is small. It indicates that the disorder induced by the highly irregular shape of the Dy "substrate" can cancel the dichroism that originates from the electronic asymmetry at the surface. The dichroism reported in earlier figures is much stronger, which is caused by the interplay of the ordering induced by the single-crystal surface, and the crystal electric fields induced by the asymmetric charge distribution around the adsorbed atoms.

To study both surface and substrate-overlayer regions of the overlayer we have evaporated a layer of Ho (a neighbor of Dy in the periodic system of elements and chemically similar) on top of the Dy layer. In this experiment we covered a strongly dichroic Dy layer (depicted in Fig. 7, right panel) with 0.5-ML Ho. This was done by evaporation of 0.5-ML Ho on top of the strongly dichroic Dy layer depicted in Fig. 7, right panel. Because of our definition of a monolayer, this amount of material is sufficient to cover the substrate surface.[42] The substrate was kept at 50 K during evaporation.

We are interested in the origins of the dichroism and we have therefore chosen these amounts of Dy and Ho to yield the best dichroic signal. We are aware that in the process we have given up the ability to make a clear distinction between the surface region and the overlayer-substrate regions. We could have made a much better distinction using a larger Dy layer, but as Figs. 8 and 9 indicate, this also involves a large loss in dichroism.

Because of the low temperatures, not much ordering can take place in the Ho layer that has been evaporated on top of the Dy/Ni substrate. Hence, not much dichroism is expected for the Ho overlayer. This is illustrated in the upper part of Fig. 10.

The Ho overlayer behaves as expected. For the Dy layer, which is now sandwiched between Ni(110) and Ho, it is very difficult to predict what the dichroism will be. The least that can be said is that the charge distribution now is modified with respect to the situation before evaporation, since Ho will contribute charge density at the side where there was vacuum before. However, the influence of the CF on the Dy ions will depend on the local environment, details of which are not known. The overall influence can be interpreted from the Dy $M_5$ spectra that were obtained after deposition of Ho. These are given in Fig. 11. In this figure, we have also included the Dy $M_5$ edge from the annealed Dy overlayer on which the Ho was evaporated to allow for comparison of the spectra before and after Ho deposition.

It is immediately apparent from Fig. 11 that the "sign" of the dichroism has changed. The 1296-eV peak previously showed a maximum at normal incidence, and a minimum at grazing incidence. After evaporation of Ho this situation is reversed. This means that the averaged orientation of the total angular momentum $J$ of the Dy

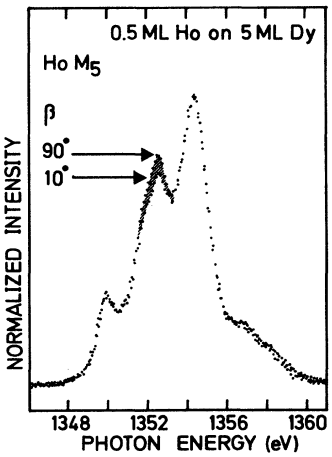


FIG. 9. The dichroism spectra as obtained for an overlayer system consisting of 5-ML Dy, with half a monolayer of Ho deposited on top. The Ho $M_5$ spectra are shown for normal incidence ($\beta = 90°$) and grazing incidence ($\beta = 10°$). Deposition and subsequent measurements were performed at room temperature.

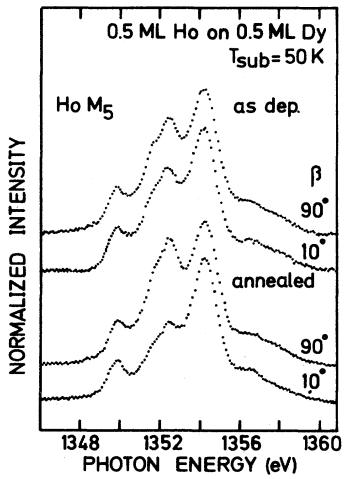


FIG. 10. 0.5-ML Ho evaporated onto the annealed overlayer of 0.5-ML Dy on Ni(110) showing large dichroism. In this figure the Ho $M_5$ edge is depicted. Upper part: normal incidence ($\beta = 90°$) and grazing incidence ($\beta = 10°$) spectra for the as-deposited layer of Ho. Lower part: $\beta = 90°$ and $\beta = 10°$ spectra after annealing the overlayer system.

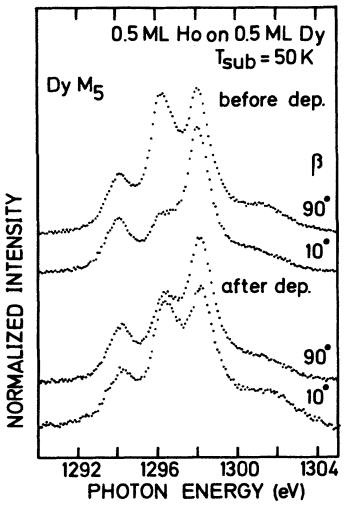


FIG. 11. 0.5-ML Ho evaporated onto the annealed overlayer of 0.5-ML Dy on Ni(110) showing large dichroism. In this figure the Dy $M_5$ edge is depicted. Upper part: normal incidence ($\beta = 90°$) and grazing incidence ($\beta = 10°$) spectra for the annealed Dy overlayer on Ni(110). Lower part: $\beta = 90°$ and $\beta = 10°$ spectra after deposition of Ho on top of the Dy overlayer.

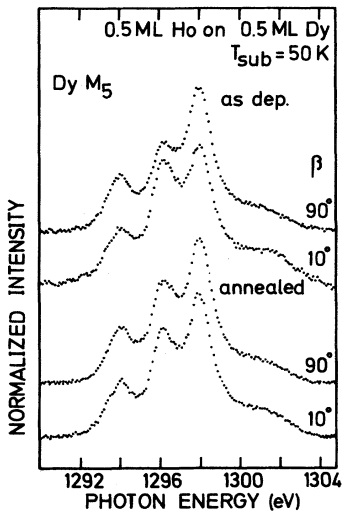


FIG. 12. 0.5-ML Ho evaporated onto the annealed overlayer of 0.5-ML Dy on Ni(110) showing large dichroism. Here the Dy $M_5$ edge is depicted. Upper part: normal incidence ($\beta = 90°$) and grazing incidence ($\beta = 10°$) spectra for the as-deposited layer of Ho. Lower part: $\beta = 90°$ and $\beta = 10°$ spectra after annealing the overlayer for 1 min at 300 °C.

ions has changed from in plane to out of plane. Analysis of the magnitude of the dichroism reveals that it has decreased upon adsorption of Ho. Therefore, either the reversal is not complete, or the nature of the crystal-field interaction (e.g., the symmetry felt by the Dy ions) has changed. It should be noted that the above picture is probably a simplification of the actual situation, since we have treated all Dy ions alike, and differences in the chemical environment for Dy atoms probably exist.

An important conclusion is obtained: the dichroism of the Dy layer (the "substrate-overlayer interface") is different from that of the Ho layer (the "overlayer-vacuum interface"). This is due to the different electronic environments felt by the ions in the two layers. Using these results for the interpretation of the dichroism thickness dependence we conclude the following: the "dilution" of the signal of active layers by nondichroic layers is still a workable model, as long as it is realized that the dichroic layers do not necessarily have identical effects, but can actually be counteractive. In particular, the observations made here give an indication why the dichroic signal falls off rapidly within the monolayer thickness regime:[42] for thicknesses between 0.5 ML and 1 ML there will be areas in the overlayer that consist of more than one layer, and the dichroism stemming from subsequent layers can be different, leading to a decrease in the observed overall dichroism. For thicker layers the hypothesis that the RE between interfacial and surface region is nondichroic might well hold.

Finally, in the lower panels of Figs. 10 and 12 the spectra obtained from the annealed Ho/Dy/Ni(110) overlayer system are depicted. The main result of this experiment was that the dichroism obtained from Dy diminished, but it did not vanish, and the orientation of the spectra was still the same as before the annealing, i.e., different from the Dy on Ni(110) spectra. The dichroism of Ho was found to increase in this experiment. Apparently, the annealing process is a driving force for the angular momenta to align in the plane of the surface. Since the Ho moments were already pointing in this direction before annealing, this leads to an increased dichroic effect. The average Dy angular momentum on the other hand was pointing out of plane. This is counteracted by the annealing process; the result is a diminished dichroism.

## VII. SUMMARY AND CONCLUDING REMARKS

In this paper we have presented linear dichroism experiments on RE (mainly Dy) overlayers on Ni(110) and Cu(110). We have shown that the strong linear dichroism, indicative of a split ground state, is due to a CF splitting. We conclude that the crystal field is such that a simple axial CF model does not suffice for a quantitative description of the results.

We propose a model in which the magnitude of the dichroism depends on the bonding of the adsorbing atoms to the surface. The stronger the bonds, the less free the adatoms are to move around and establish a more uniform environment for all adatoms and thus increase dichroism. Dichroism is strongest if the environment of the RE ions is uniform. In our experiments the best situation in this respect occurs for a single-crystal surface at elevated temperatures. At low temperatures, the RE ions may not have sufficient energy to overcome an activation energy barrier to relax to a configuration where the RE ions overall are situated in a more uniform environment. In such a situation, the dichroism will be small. Our model is able to explain why the dichroism of Dy on Ni(110) increases strongly upon annealing.

Finally, we investigated the contributions of the surface and the overlayer-substrate interface to the dichroism signal. In an experiment using a Ho probing layer we found that dichroism from these regions may be counteractive. The result is that the magnitude of the dichroism starts decreasing before the first layer of RE ions is completed.

## ACKNOWLEDGMENTS

We are grateful to L. Schreurs and J. Hermsen for the preparation of the Ni(110) and Cu(110) single crystals and B.T. Thole for the Dy multiplet calculations. This work has been supported in part by the Stichting voor Fundamenteel Onderzoek der Materie (FOM) and the Stichting Scheikundig Onderzoek in Nederland (SON) with financial support from the Nederlandse Stichting voor Wetenschappelijk Onderzoek (NWO), and by the Committee for the European Development of Science and Technology (CODEST) program. The Laboratoire pour l'Utilisation du Rayonnement Électromagnétique is a Laboratoire Propre du Centre National de la Recherche Scientifique.

*Deceased.

[1]P. Zeeman, Philos. Mag. **43**, 226 (1897); **44**, 55 (1897); **44**, 255 (1897).

[2]J.L. Erskine and E.A. Stern, Phys. Rev. B **12**, 5016 (1975).

[3]E. Keller and E.A. Stern, *EXAFS and Near Edge Structure III* (Springer, Berlin, 1984).

[4]B.T. Thole, G. van der Laan, and G.A. Sawatzky, Phys. Rev. Lett. **55**, 2086 (1985).

[5]G. van der Laan, B.T. Thole, G.A. Sawatzky, J.B. Goedkoop, J.C. Fuggle, J.-M. Esteva, R. Karnatak, J.P. Remeika, and H.A. Dabkowska, Phys. Rev. B **34**, 6529 (1986).

[6]J.B. Goedkoop, M. Grioni, and J.C. Fuggle, Phys. Rev. B **43**, 1179 (1991).

[7]G. Schütz, W. Wagner, W. Wilhelm, P. Kienle, R. Zeller, R. Frahm, and G. Materlik, Phys. Rev. Lett. **58**, 737 (1987).

[8]G. Schütz, M. Knülle, R. Wienke, W. Wilhelm, W. Wagner, P. Kienle, and R. Frahm, Z. Phys. B **73**, 67 (1988).

[9]R.J.H. Kappert, M. Sacchi, J.B. Goedkoop, M. Grioni, and J.C. Fuggle, Surf. Sci. **248**, L245 (1991).

[10]M. Sacchi, O. Sakho, and G. Rossi, Phys. Rev. B **43**, 1276 (1991).

[11]G. Schütz, R. Frahm, P. Mautner, R. Wienke, W. Wagner, W. Wilhelm, and P. Kienle, Phys. Rev. Lett. **62**, 2620 (1989).

[12]L. Baumgarten, C.M. Schneider, H. Petersen, F. Schäfers, and J. Kirschner, Phys. Rev. Lett. **65**, 492 (1990).

[13]F. Baudelet, C. Brouder, E. Dartyge, A. Fontaine, J.P. Kappler, and G. Krill, Europhys. Lett. **13**, 751 (1990).

[14]F. Baudelet, E. Dartyge, A. Fontaine, C. Brouder, G. Krill, J.P. Kappler, and M. Piecuch, Phys. Rev. B **43**, 5857 (1991).

[15]C.T. Chen, N.V. Smith, and F. Sette, Phys. Rev. B **43**, 6785 (1991).

[16]M. Sacchi, O. Sakho, F. Sirotti, X. Jin, and G. Rossi, Surf. Sci. **251/252**, 346 (1991).

[17]M. Sacchi, O. Sakho, F. Sirotti, and G. Rossi, Appl. Surf. Sci. **56/58**, 1 (1992).

[18]J.B. Goedkoop, B.T. Thole, G. van der Laan, G.A. Sawatzky, F.M.F. de Groot, and J.C. Fuggle, Phys. Rev. B **37**, 2086 (1988).

[19]H. Ebert, P. Strange, and B.L. Gyorffy, Z. Phys. B **73**, 77 (1988).

[20]H. Ebert, B. Drittler, R. Zeller, and G. Schütz, Solid State Commun. **69**, 485 (1989).

[21]P. Carra and M. Altarelli, Phys. Rev. Lett. **64**, 1286 (1990).

[22]J.B. Goedkoop, J.C. Fuggle, B.T. Thole, G. van der Laan, and G.A. Sawatzky, J. Appl. Phys. **64**, 5595 (1988).

[23]T. Jo and S. Imada, J. Phys. Soc. Jpn. **58**, 1922 (1989); **59**, 2312 (1990).

[24]S. Imada and T. Jo, J. Phys. Soc. Jpn. **59**, 3358 (1990).

[25]G. van der Laan and B.T. Thole, Phys. Rev. B **42**, 6670 (1990).

[26]C. Brouder and M. Hikam, Phys. Rev. B **43**, 3809 (1991).

[27]P. Carra, B.N. Harmon, B.T. Thole, M. Altarelli, and G.A. Sawatzky, Phys. Rev. Lett. **66**, 2495 (1991).

[28]T. Jo and G.A. Sawatzky, Phys. Rev. B **43**, 8771 (1991).

[29]G. van der Laan and B.T. Thole, Phys. Rev. B **43**, 13 401 (1991).

[30]J.B. Goedkoop, Ph.D. thesis, University of Nijmegen, 1989.

[31]U. Fano, Phys. Rev. **178**, 131 (1969); **184**, 250 (1969).

[32]B.T. Thole, G. van der Laan, J.C. Fuggle, G.A. Sawatzky, R.C. Karnatak, and J.-M. Esteva, Phys. Rev. B **32**, 5107 (1985).

[33]R.J.H. Kappert, Ph.D. thesis, University of Nijmegen, 1992.

[34]Extra support for the interpretation of the observed dichroism in terms of electrostatic fields is given by M. Sacchi, F. Sirotti, G. Rossi, R.J.H. Kappert, J. Vogel, and J.C. Fuggle, J. Electron Spectrosc. Relat. Phenom. **58**, 393 (1992), who showed that *circular* dichroism is absent in Dy deposited on a magnetic FeNiB substrate. The absence of circular dichroism and the presence of a strong linear dichroic effect can be regarded as a fingerprint of crystal-field effects (Ref. 33, Chap. 2).

[35]The spectra depicted in Fig. 4 have been taken from an earlier study (see Ref. 9). The remanent magnetism of the Ni crystal in the present study is 20% higher, but the data obtained show no significant differences with the spectra depicted in Fig. 4.

[36]D. Lagraffe, P.A. Dowben, and M. Onellion, Phys. Rev. B **40**, 3348 (1989); J. Vac. Sci. Technol. A **8**, 2738 (1990).

[37]A. Nilsson, B. Eriksson, N. Mårtensson, J.N. Andersen, and J. Onsgaard, Phys. Rev. B **38**, 10 357 (1988).

[38]I. Chorkendorff, J. Onsgaard, J. Schmidt-May, and R. Nyholm, Surf. Sci. **160**, 587 (1985).

[39]J.N. Andersen, J. Onsgaard, A. Nilson, B. Eriksson, E. Zdansky, and N. Mårtenson, Surf. Sci. **189/190**, 399 (1987).

[40]A.R. Miedema, P.F. de Châtel, and F.R. de Boer, Physica B **100**, 1 (1980).

[41]We also found that Dy disappears from the substrate upon annealing of the substrate. This was particularly noticeable for the Cu surface, which is another indication of the higher mobility of the Dy atoms over the Cu surface.

[42]Our definition of a monolayer is related to the rare-earth metal (see Sec. II). In these terms, 0.5-ML Dy on Ni(110) is sufficient material to cover the substrate surface.